

CRYSTAL-FIELD SPECTRA OF CHRYSOBERYL,  
ALEXANDRITE, PERIDOT, AND SINHALITE<sup>1</sup>E. F. FARRELL AND R. E. NEWNHAM, *Electrical Engineering  
Dept., M.I.T.*

## ABSTRACT

The optical absorption spectra of the isomorphous minerals chrysoberyl, alexandrite, peridot, and sinhalite have been measured in polarized light at 77° K. Electronic transitions between the  ${}^6A_1$  ground state of  $\text{Fe}^{3+}$  and a number of quartet states give rise to the color of yellow chrysoberyl. The broad absorption bands of alexandrite are due to the  ${}^4A_2 \rightarrow {}^4T_2$  and  ${}^4A_2 \rightarrow {}^4T_1$  excitations of octahedrally coordinated  $\text{Cr}^{3+}$ . Sinhalite and peridot show intense absorption near  $1\ \mu$ , caused by the  ${}^5T_2 \rightarrow {}^5E$  transition of  $\text{Fe}^{2+}$ .

## INTRODUCTION

Chrysoberyl ( $\text{Al}_{2-x}\text{Fe}_x\text{BeO}_4$ ), alexandrite ( $\text{Al}_{2-x}\text{Cr}_x\text{BeO}_4$ ) peridot ( $\text{Mg}_{2-x}\text{Fe}_x\text{SiO}_4$ ), and sinhalite ( $\text{Al}_{1-x}\text{Mg}_{1-y}\text{Fe}_{x+y}\text{BO}_4$ ) are gem minerals belonging to the olivine family. Their distinctive colors and optical absorption spectra are caused by small concentrations of iron and chromium. Although often used in identification (Smith, 1962; Webster, 1962), no adequate interpretation of the spectra has been published.

The olivine structure, first established by Bragg and Brown (1926), is based on a hexagonal close-packed array of oxygen ions. Within this framework, one eighth of the tetrahedral interstices are occupied by Si, Be or B, whereas larger cations, such as Al, Mg, Fe and Cr, fill half the octahedral sites. Recent structure refinements of chrysoberyl (Farrell *et al.*, 1963), olivine (Hanke and Zemann, 1963), and sinhalite (Fang and Newnham, 1965) revealed certain minor distortions but confirmed the basic arrangement. The iron and chromium environments are of particular importance in understanding the absorption spectra. Although the near-neighbor coordination resembles an octahedron, the true symmetry of the two transition-metal sites ( $\bar{1}$  and  $m$ ) is much lower. The departures from octahedral symmetry ( $m3m$ ) will be neglected in the discussion which follows, though some relaxation of the selection rules and line-splitting might be expected to result.

Electronic energy-level diagrams for  $\text{Cr}^{3+}$ ,  $\text{Fe}^{3+}$ , and  $\text{Fe}^{2+}$  in octahedral coordination are shown in Fig. 1. The optical absorption spectra involve the redistribution of electrons in the partially filled  $3d$  shell, transitions that violate the Laporte selection rule. Lattice vibrations and acentric distortions lead to a mixing of  $d$  and  $p$  orbitals, so that transitions forbidden to the free ion may occur with low intensity in the solid state.

The energy-level diagrams are based on quantum-mechanical calcula-

<sup>1</sup> Sponsored by Advanced Research Projects Agency, Contract SD-90, and by the U. S. Air Force, Aeronautical Systems Division, under Contract AF 33 (615)-2199.

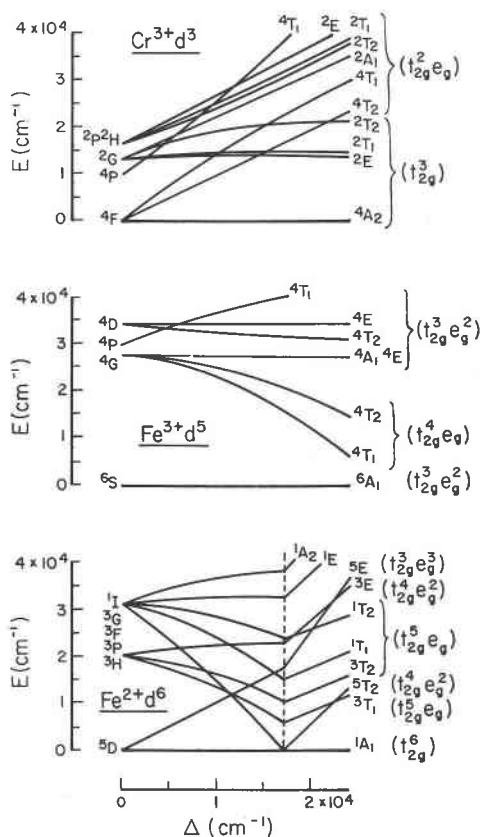


FIG. 1. Energy-level diagrams for octahedrally coordinated  $\text{Cr}^{3+}$ ,  $\text{Fe}^{3+}$  and  $\text{Fe}^{2+}$ , plotted as a function of the crystal-field parameter  $\Delta$ .

tions by Tanabe and Sugano (1954), revised and extended by others (McClure, 1959 and Griffith, 1962). An introductory account of crystal-field theory, defining most of the terms used in this article, has been written by Orgel (1960). To the left of each diagram ( $\Delta=0$ ) lie the electronic states of the free ion. Hund's rule regarding maximum spin determines the ground state, and the excitation energies for higher states are derived from spectroscopic data. When an octahedral arrangement of anions surrounds the transition-metal atom, the  $d$  orbitals split into  $t_{2g}$  and  $e_g$  orbitals. The lower-lying  $t_{2g}$  orbitals point between the anions and are triply-degenerate ( $d_{xy}$ ,  $d_{xz}$ ,  $d_{yz}$ ). The electron density of the  $e_g$  orbitals ( $d_{x^2-y^2}$ ,  $d_{z^2}$ ) is concentrated near the anions, raising their energy through Coulomb repulsion. The strong-field configurations adopted by each electronic state are given in parentheses on the far right. Mulliken symmetry notation is used to designate states in the intermediate range. A large

crystal field will sometimes convert the ground state to a low-spin configuration, as shown in the  $\text{Fe}^{2+}$  diagram.

Tentative assignments for the spectra observed in olivine-family minerals are given in succeeding sections. Comparable spectra for other inorganic compounds and for ions in solution are summarized by Jørgenson (1962).

#### EXPERIMENTAL

Absorption spectra between 0.2 and 2.0  $\mu$  were recorded on an extended-range Beckman DK-1 spectrophotometer using a calcite air-gap prism as a polarizer. A polarizing microscope and back-reflection Laue camera were used to orient the specimens, which were subsequently cut into plates with a diamond saw and polished with diamond paste. Cooling the specimens to 77° K in a liquid-nitrogen cryostat gave improved spectral resolution over room-temperature measurements.

Figures 3-7 plot the absorption coefficient  $\alpha$  as a function of wavelength and wavenumber, a convenient measure of energy.  $\alpha$  is defined by Lambert's Law as  $(1/t) \log_e (I_0/I)$ , where  $t$  is the sample thickness and  $I_0$  and  $I$  are the incident and transmitted intensities, respectively. No corrections were applied for scattered or reflected light. Vibration directions were chosen in accordance with space group *Pnma* in which, for example, the lattice parameters of chrysoberyl are  $a=9.40$ ,  $b=5.48$  and  $c=4.43$  Å.

Ultraviolet absorption-edge measurements were made on pure  $\text{Al}_2\text{BeO}_4$ , using small platelets grown by flux fusion (Farrell and Fang, 1964). Their fragility precluded polishing, and the resulting scattered light led to high optical density. Unpolarized light was used because the absorption edge of undoped chrysoberyl lies beyond the range of the calcite prism. As shown in Fig. 2, the charge-transfer bands commence at 0.2  $\mu$  (6 eV), with a tail extending to  $\sim 0.4$   $\mu$  (3 eV). The electrical conductivity data reported by Weir and Van Valkenburg (1960) gave a thermal energy gap of 2.4 eV, close to the optical threshold. It is therefore likely that electronic excitations in the 3- to 6 eV range are accompanied by phonon absorption, and direct transitions between the valence and conduction bands begin at 6 eV.

#### ALEXANDRITE

The optical absorption spectra of synthetic and natural alexandrite are shown in Figs. 3 and 4. Thin, pseudohexagonal platelets of chromium-doped  $\text{Al}_2\text{BeO}_4$  were grown by the flux-melt method using lithium molybdate as a solvent (Farrell and Fang, 1964). Absorption measurements for the *c*-polarization direction proved impracticable because of the crystal morphology. The data collected for the *a* and *b* directions (Fig. 3 and Table 1) are typical of trivalent chromium in octahedral coordination.

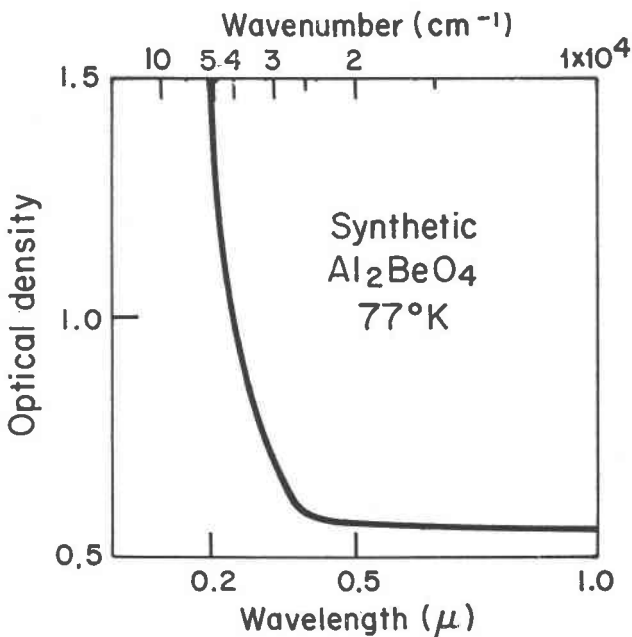


FIG. 2. The absorption edge of undoped  $\text{Al}_2\text{BeO}_4$ .

Intense absorption bands occur at  $0.6$  and  $0.4 \mu$ , and near the absorption edge at  $0.3 \mu$ . These are spin-allowed transitions from the  $^4A_2$  ground state to  $^4T_2(F)$ ,  $^4T_1(F)$  and  $^4T_1(P)$ . Using Fig. 1, a value of  $1700 \text{ cm}^{-1}$  was obtained for the crystal field parameter,  $\Delta$ . The breadth of these bands is connected with the Franck-Condon principle. Since the spatial configuration of the electronic ground state differs from that of the excited states, optical excitation is accompanied by vibrational excitation. The vibrational states scarcely differ in energy and, except at low temperatures, result in a single broad band. The subsidiary maxima at  $0.61$ ,  $0.62$ , and  $0.64 \mu$  are manifestations of the vibrational structure.

Several weak spin-forbidden transitions occur near  $0.68$  and  $0.47 \mu$ . Under high resolution these lines are extremely narrow, similar to the "R" and "B" lines of ruby. They are identified with transitions from the  $^4A_2$  ground state to the  $^2E$ ,  $^2T_1$  and  $^2T_2$  doublet states. Changes in spin orientation take place during the transitions, but the spatial configuration remains unaltered; hence, the spectra are weak but sharp. Transitions to higher doublet states (predicted near  $0.3 \mu$  from Fig. 1) are difficult to observe. Both the spatial and spin configurations change, giving rise to only broad, feeble absorption.

The natural alexandrite specimen (Fig. 4) originated from the Ural Mts. The measured density is  $3.722$ , approximating a composition

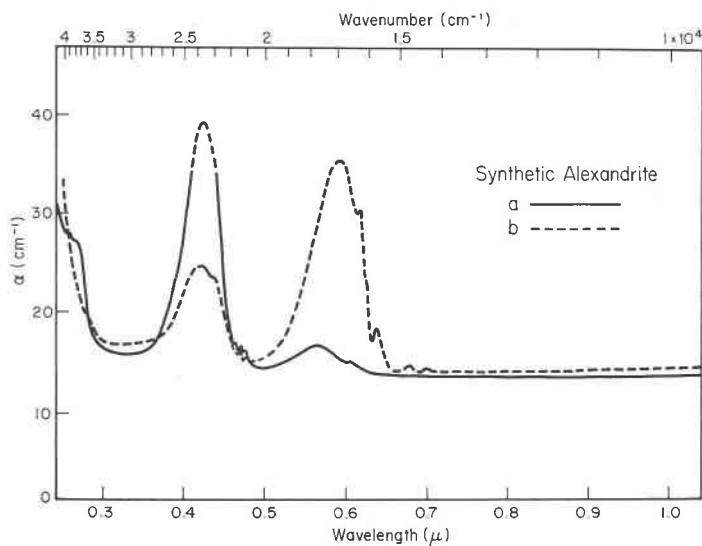


FIG. 3. Absorption spectrum of synthetic alexandrite in polarized light at 77° K.

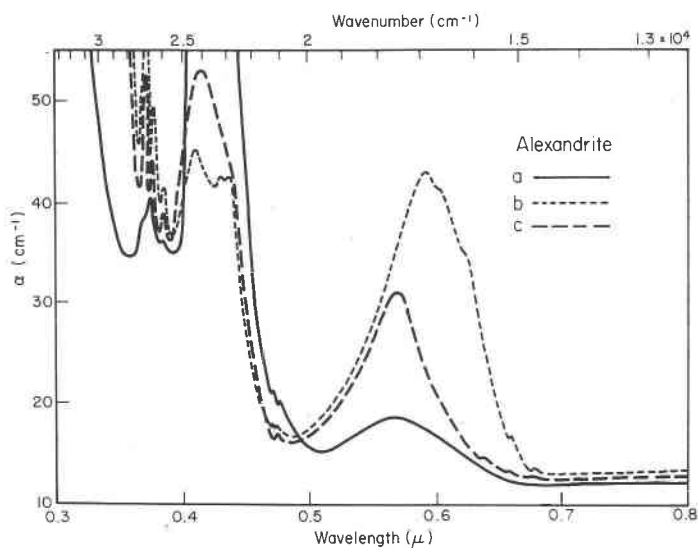


FIG. 4. Absorption spectrum of natural alexandrite in polarized light at 77° K.

TABLE 1. PRINCIPAL ABSORPTION SPECTRA OF THE OLIVINE-FAMILY MINERALS. WAVELENGTHS FOR THE THREE POLARIZATION DIRECTIONS ARE EXPRESSED IN MICRONS. PARTIALLY RESOLVED ABSORPTION PEAKS ARE BRACKETED, AND ASTERISKS DENOTE UNRESOLVED SHOULDERS

Chrysoberyl			Alexandrite			Synthetic Alexandrite			Peridot			Sinhaitite		
a	b	c	a	b	c	a	b		a	b	c	a	b	c
.355	.355	.355				.255	.285		.395	.395	.410	.380	.380	.390
.366	.367	.367		.368	.368	.265			.410	.410	.430	.390	.390	.400
.368										.430	.425*	.410*	.410*	.400
.377	.375*	.376*							.455	.460	.450	.450	.450	.445
.378	.376	.377		.378	.378				.475	.470	.455	.460	.460	.450
.379									.490	.485	.460	.490*	.490*	.460
.383	.382	.382		.385	.385				.500	.500	.475			
.384	.384	.383		.410	.410				.525*	.510	.485		.490	
	.438	.441		.430	.430*	.425	.425				.495	.525	.525	.525
				.440	.440		.440		.640	.640	.500	.670	.670	.670
						.465	.470				.640			
	.500			.470	.470	.470	.470		.860	.860		.960*	.925	
	.615			.475	.475	.475	.475							
				.560	.595	.565	.595		1.07	1.07	1.07	1.07	1.05	1.07
1.00				.605	.605	.605	.610							
				.620	.620	.620	.620		1.30*	1.30*		1.14		
				.645	.645		.640							
				.660	.660									
				.680	.680		.680							
							.700							

$\text{Al}_{1.96}(\text{Cr}, \text{Fe})_{0.04}\text{BeO}_4$ . Crystal field spectra of trivalent iron and chromium are readily identified by comparison with Figs. 3 and 5. The origin of the iron spectra at 0.368, 0.378, 0.385 and 0.44  $\mu$  will be discussed later. Chromium causes remarkable pleochroism in alexandrite; the colors are yellow, green, and red for light polarized along  $a$ ,  $b$  and  $c$ , respectively. An intense absorption in the dark blue (0.42  $\mu$ ) dominates the  $a$  spectrum, giving transmitted light its complementary color, yellow. Blue is again absorbed in the  $b$  and  $c$  spectra, but the transmitted colors are also influenced by the band near 0.6  $\mu$ . The latter absorbs yellow for  $c$ , and both red and yellow for  $b$ . As a result, red is the dominant  $c$  color, while only green radiation (0.5  $\mu$ ) is transmitted for light polarized parallel to  $b$ .

Neuhaus (1960) has correlated the absorption bands and color of many chromium-bearing oxides. Wavelengths of 0.58 and 0.415  $\mu$  prove critical for the  ${}^4A_2 \rightarrow {}^4T_2$  and  ${}^4A_2 \rightarrow {}^4T_1$  transitions. If the absorption bands exceed these values, the substance is green; otherwise it is red. The principal absorption bands of alexandrite straddle the critical values, ranging from 0.565 to 0.595 and from 0.41 to 0.42  $\mu$  (Table 1). A natural consequence is its unique coloring: green by daylight and red under ordinary incandescent illumination. The spectrum of sunlight corresponds to a black-body radiator of 6000° K with an intensity maximum in the green (0.5  $\mu$ ). The "window" between the principal absorption bands of alexandrite transmits this color, giving the crystal a green appearance in daylight. Longer wavelengths predominate in incandescent light (2400° K), and the red color results from transmission near 0.7  $\mu$ .

#### CHRYSOBERYL

Ferric iron gives rise to the crystal-field spectra of yellow chrysoberyl (Fig. 5). Absorption measurements were made on a Brazilian specimen having a composition  $\text{Al}_{1.96}\text{Fe}_{0.04}\text{BeO}_4$  and a specific gravity of 3.720. Appreciable absorption occurs only in the blue-violet portion of the visible spectrum; hence, the crystal appears yellow, the complementary color. The spectra are nearly identical in the three polarization directions, showing little or no pleochroism.

The trivalent iron spectrum is due to spin-forbidden transitions from the  ${}^6A_1$  ground state to excited quartets (cf. Fig. 1) and is therefore weak. Transitions to  ${}^4T_1(G)$  and  ${}^4T_2(G)$ , the two lowest levels, are very broad and barely observable at 0.615 and 0.50  $\mu$ . Their breadth can be explained by the Franck-Condon principle since electrons shift from  $e_g$  to  $t_{2g}$  orbitals during the transitions. A series of sharper spectra between 0.44 and 0.355  $\mu$  is probably due to the  ${}^4A_1(G)$ ,  ${}^4E(G)$ ,  ${}^4T_2(D)$  and  ${}^4E(D)$  states. These transitions occur entirely within the  $t_{2g}^3 e_g^2$  spatial configuration. Quantitative agreement between the observed spectra and the  $d^5$  energy-level diagram in Fig. 1 can only be achieved by reducing the energy

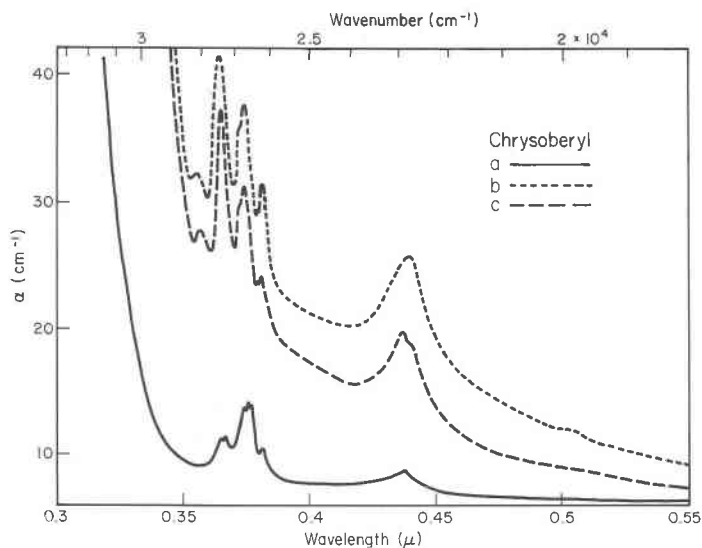


FIG. 5. Absorption spectrum of chrysoberyl in polarized light at 77° K.

separation of the excited states relative to the ground state. Similar reductions in other ferric iron oxides have been attributed to covalent bonding between the metal ion and neighboring anions (Wickersheim and Lefever, 1962). The weak absorption observed at  $1\ \mu$  in chrysoberyl is probably caused by divalent iron.

#### PERIDOT AND SINHALITE

The absorption spectra of peridot (olivine proper) and sinhalite are very similar (Figs. 6 and 7), contributing to the problem of distinguishing between the two minerals. Our peridot specimen had a density of 3.361, composition  $\text{Mg}_{1.75}\text{Fe}_{0.25}\text{SiO}_4$ , and was mined in Arizona. The sinhalite from Ceylon had a density of 3.494, corresponding to a composition  $(\text{Al}, \text{Mg})_{1.95}\text{Fe}_{0.05}\text{BO}_4$ . Judging from the absorption data, most of the iron in sinhalite is divalent, like that of peridot.

The salient feature of both absorption curves is an intense peak near  $1\ \mu$ . Assuming  $\text{Fe}^{2+}$  adopts the  ${}^5T_2$  ground state in accordance with Hund's rules, the only spin-allowed transition is to  ${}^5E$ . The  $d^6$  diagram in Fig. 1 gives  $\Delta = 10,000\ \text{cm}^{-1}$ . Much of the broadness can be attributed to the change in spatial configuration ( $t_{2g}^4e_g^2$  to  $t_{2g}^3e_g^3$ ), but the Jahn-Teller effect also deserves consideration. Jahn-Teller distortions in octahedrally coordinated  $\text{Fe}^{2+}$  are due to asymmetrical occupation of the  $t_{2g}$  orbitals, leading to asymmetric interatomic forces which in turn create spectral separations.



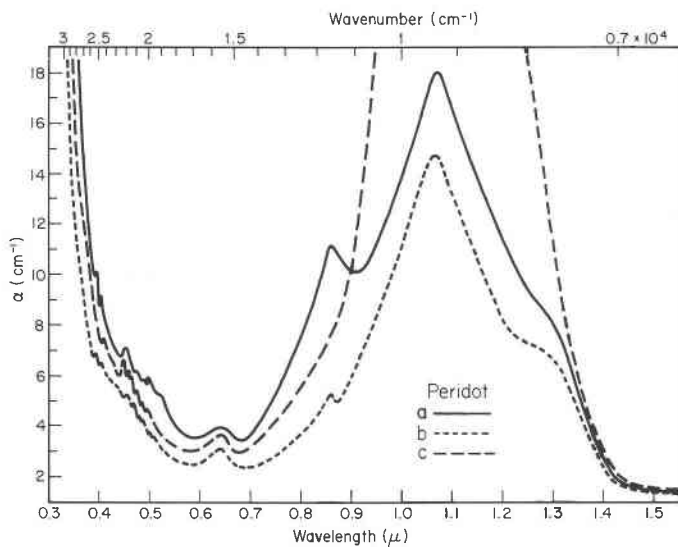


FIG. 6. Absorption spectrum of olivine in polarized light at 77° K.

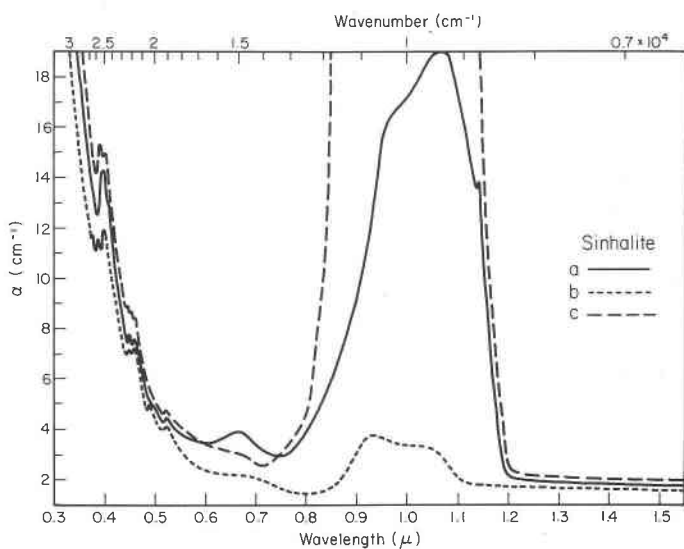


FIG. 7. Absorption spectrum of sinhalite in polarized light at 77° K.

A number of weaker spectra were observed between 0.35 and 0.65  $\mu$ . These originate from spin-forbidden transitions between the quintet ground state and excited triplets. Conclusive identification of these spectra requires a more complete energy-level diagram than is presently available.

Since there are no intense spectra in the visible, the characteristic colors of peridot (green) and sinhalite (olive-brown) must originate from absorption bands in the near ultraviolet and near infrared. The tail of the 1 $\mu$  band in peridot extends to 0.7  $\mu$ , absorbing much of the red; thus transmitted light appears green, the complementary color. The absorption spectra in sinhalite are shifted to longer wavelengths, making the absorption edge in the near ultraviolet more important. Neither crystal shows pronounced pleochroism.

#### ACKNOWLEDGMENTS

We wish to thank our associates in the M.I.T. Materials Science Center for their advice and assistance with the experiments.

#### REFERENCES

- BRAGG, W. L. AND G. B. BROWN (1926) Die Kristallstruktur von Chrysoberyl ( $\text{BeAl}_2\text{O}_4$ ). *Zeit. Krist.* **63**, 122-143.
- FANG, J. H. AND R. E. NEWNHAM (1965) The crystal structure of sinhalite. *Mineral. Mag.* (accepted for publication).
- FARRELL, E. F. AND J. H. FANG (1964) Flux growth of chrysoberyl and alexandrite. *Jour. Am. Ceram. Soc.* **47**, 274-276.
- , J. H. FANG AND R. E. NEWNHAM (1963) Refinement of the chrysoberyl structure. *Am. Mineral.* **48**, 804-810.
- GRIFFITH, J. S. (1961) *The Theory of Transition-Metal Ions*. Cambridge University Press.
- HANKE, K. AND J. ZEMANN (1963) Verfeinerung der Kristallstruktur von Olivin. *Naturwiss.* **50**, 91-92.
- JØRGENSEN, C. K. (1962) *Absorption Spectra and Chemical Bonding in Complexes*. Pergamon Press, Ltd., London.
- MCCLURE, D. S. (1959) Electronic spectra of molecules and ions in crystals. *Solid State Physics* **9**, 399-525.
- NEUHAUS, A. (1960) Über die Ionenfarben der Kristalle und Minerale am Beispiel der Chromfärbungen. *Zeit. Krist.* **113**, 195-233.
- ORGEL, L. E. (1960) *An Introduction to Transition-Metal Chemistry: Ligand Field Theory*. Methuen & Co., Ltd., London.
- SMITH, G. F. H. (1962) *Gemstones*. Pitman, New York.
- TANABE, Y. AND S. SUGANO (1954) On the absorption spectra of complex ions. *Jour. Phys. Soc. Japan* **9**, 753-779.
- WEBSTER, R. (1962) *Gems: Their Sources, Descriptions, and Identification*. 2 Vols. Butterworths, London.
- WEIR, C. E. AND A. VAN VALKENBURG (1960) Studies of beryllium chromite and other beryllia Compounds with  $\text{R}_2\text{O}_3$  oxides. *Jour. Res. N.B.S.* **64A**, 103-106.
- WICKERSHEIM, K. A. AND R. A. LEFEVER (1962) Absorption spectra of ferric iron-containing oxides. *Jour. Chem. Phys.* **36**, 844-850.

*Manuscript received, March 15, 1965; accepted for publication, September 9, 1965.*